

## CHAPTER 168

### Abrasion of Steel Pipe Piles by Sediment Motion in Coastal Zones

Gaku Matsuoka<sup>1</sup>, Shinichi Ito<sup>2</sup>, Toshihiko Yamashita<sup>3</sup>  
Hiroshi Saeki<sup>4</sup>, Yoshihisa Kariyazono<sup>5</sup>, and Koichi Sato<sup>6</sup>

#### ABSTRACT

In the outer coastal zones, where wave conditions are severe, steel-pipe piles often undergo abrasion due to the collision of sand particles. The abrasion characteristics of steel-pipe piles were clarified from the results of full-scale experiments. The abrasion rate of steel-pipe piles was found to be approximately proportional to the second power of the amplitude of flow velocity. The larger the ratio of sand particle diameter to pile diameter was, the higher was the abrasion rate. As the collision energy of sand particles obtained by numerical analysis was nearly proportional to the measured abrasion rate, it was considered that the abrasion rate can be estimated from the collision energy.

#### INTRODUCTION

Large amounts of sand particles sometimes drift around pipe piles due to the action of waves, especially in outer coastal zones. Steel-pipe piles exposed to these drifting sand particles undergo abrasion due to the collision of sand particles with the piles. Durability is an important consideration in the construction of steel structures in coastal zones. Culbertson W. Ross (1949) reported severe abrasion and corrosion of

- 
- 1) Graduate Student, Dept. of Civil Engineering, Hokkaido University, Kita-13 Nishi-8 Sapporo 060 JAPAN
  - 2) Civil Engineer, Niigata Prefectural Government, 4-1 Sinkoucho Niigata 950-70 JAPAN
  - 3) Associate Professor, Dept. of Civil Engineering, Hokkaido University, Ditto
  - 4) Professor, Dept. of Civil Engineering, Hokkaido University, Ditto
  - 5) Senior Researcher, Kimitsu R & D Laboratories, Nippon Steel Corporation, Kimitsu-1 Kimitsu-city Chiba 299-11 JAPAN
  - 6) Senior Manager, Sapporo Sales Office, Nippon Steel Corporation, Kita-2 Nishi-4 Sapporo 060 JAPAN

steel-pile groins at Palm Beach, Florida. There have also been reports of large decreases in the wall thickness of steel-pipe piles (more than 1mm/year) due to abrasion and corrosion in other outer coastal zones. The reported rates of decrease in the wall thickness are more than 10 times greater than the allowable corrosion rate of steel in sea water (0.1mm/year). However, except for our previous studies (Yamashita et al., 1989, 1990, 1991, 1992; Kariyazono, 1992), there have been very few experimental or theoretical studies on the abrasion of steel piles due to sediment motion. The behavior of sand particles during collision with the surface of piles and the resulting abrasion of the surface have not yet been clarified.

In the present study, full-scale experiments were carried out to investigate the abrasion characteristics of steel-pipe piles from the viewpoint of the effects of flow velocity, diameter of sand particles and diameter of piles. Also, from numerical analysis of the motion of suspended sand particles, the characteristics of the collision energy of sand particles against steel piles were investigated, and the relationship between collision energy and abrasion rate was clarified.

## EXPERIMENTS

A series of abrasion tests on steel-pipe piles were carried out in the laboratory using a large-scale U-shaped tube that could generate a strong oscillatory flow with sand drift (Fig. 1). The tube is 10m in horizontal length, 5m in height and 1m in width. The horizontal part of the apparatus, which is 500mm in height, was filled with sand to a height of 400mm. Thus, the flow took place in the upper 100mm of the horizontal part. The experimental flow conditions were as follows: the period of oscillatory flow was 7.1 or 7.4 sec and the amplitude of velocity ( $u_0$ ) was 2.0m/s ~ 4.0m/s. Three sizes of pipe piles (267, 140 and 76mm in diameter( $\phi$ )), and four grades of sand (0.75, 1.5, 4.0 and 7.0mm in diameter( $d$ )) were used. The specific gravity was 2.65 in all sand particles. The steel piles, which were made of 392N/mm<sup>2</sup> carbon steel, were fixed securely to the bottom of the horizontal part of the apparatus

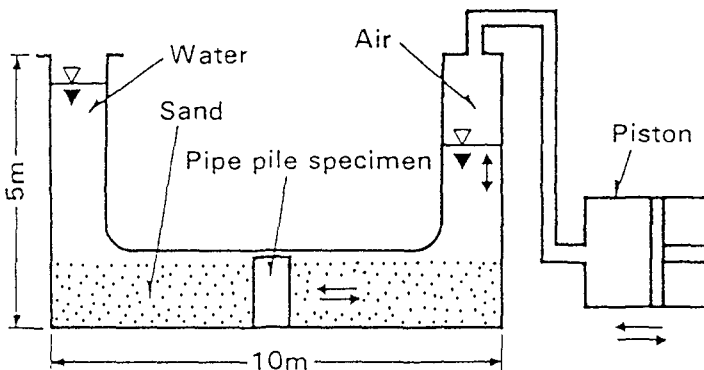


Fig. 1 Large-scale U-shaped tube that can generate a strong oscillatory flow with sand drift.

by steel caps and bolts. Rubber bands were wrapped around both ends of each steel-pipe specimen to prevent abrasion of the surface during the test. Most of the tests were carried out under conditions in which the period was 7.4 sec and the amplitudes of flow velocity were 2.0 or 3.0m/s. Flow velocity of 2.0 and 3.0m/s are equivalent to strong waves of 5.4 and 8.1m in height, respectively, which occur in coastal zones with a water depth of 10m.

Fig. 2 shows a schematic diagram of the apparatus used to measure the surface profile of each specimen. The surface profiles were measured in the longitudinal direction by a dial gage before and after each abrasion test. Surface profile measurements were carried out at intervals of 15 degrees to the main flow direction.

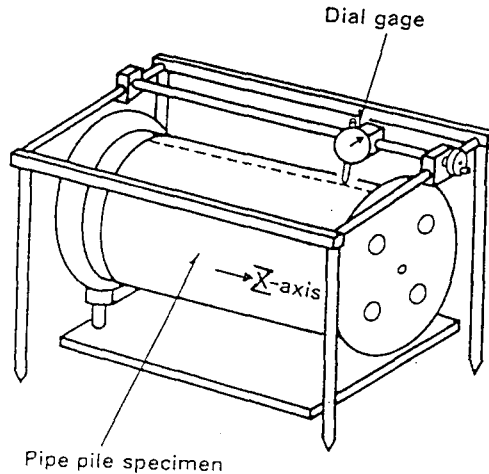


Fig. 2 Measurement of the surface profile of a pipe pile specimen.

## RESULTS and DISCUSSION

Fig. 3 shows an example of the surface profiles of a steel pipe pile before and after the abrasion test. The Z-axis is the distance from the upper standard line of the pipe (see Fig. 4). The upper and lower parts of the pile were covered with rubber bands to prevent abrasion during the test. The amount of abrasion was obtained from the difference between surface profiles before and after the test.

Fig. 4 shows an example of the profile of the sand bed around a steel pipe pile after the test at a flow velocity of 3.0m/s. The diameter of the steel pipe pile was 267 mm. The depth of the sand far from the pile was about 440mm, while but sand around the pile was scoured to a depth of about 120mm. The degree of scouring was greater at a flow velocity of 3.0m/s than at 2.0m/s.

Fig. 5 shows an example of the distributions of the amount of abrasion. The dotted lines indicate the surface of the sand bed at the pile surface. The solid lines indicate the surface of the sand bed far from the pile. At the upper part of sand bed

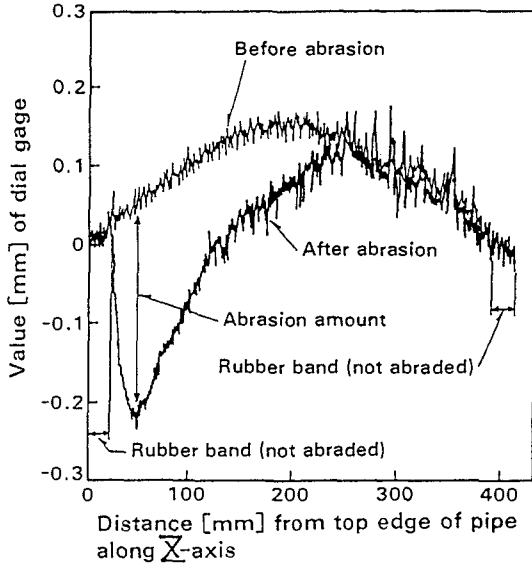


Fig. 3 Surface profiles of a specimen before and after abrasion.

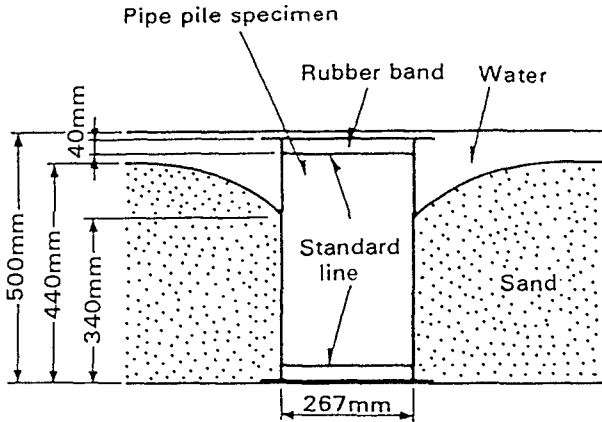


Fig. 4 Profile of the sand bed around the pipe pile specimen.

surface from the dotted line, the amount of abrasion was largest at 15 or 30 degrees and smallest at 90 degrees. The maximum amount of abrasion was observed at about 50mm above the sand bed and at 15 or 30 degrees to the main flow direction. In the

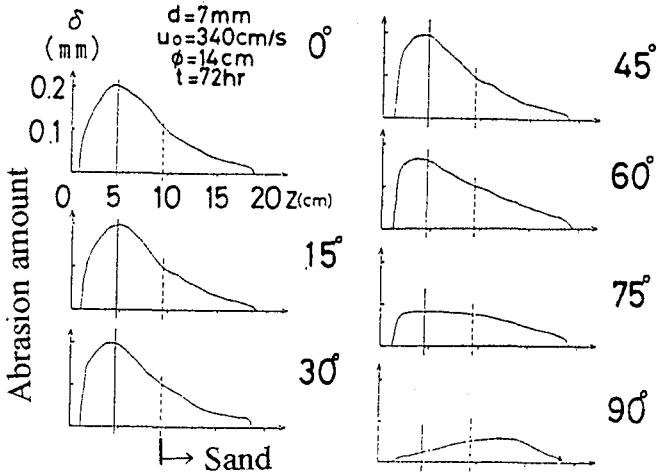


Fig. 5 Distributions of the amount of abrasion of the pile along the distance from the top standard line.

case where the sand particle diameter was 7mm and the flow velocity was 3.4m/sec, the maximum amount of abrasion was 0.2mm/3days. This value corresponds to 2mm/month. Thus, it was confirmed that a serious loss of 1mm/year in wall thickness was expected in coastal zones with severe sand motion. At the lower part of the sand bed surface, the amount of abrasion was rather small and was independent of the angle. At the upper part of the sand bed surface, abrasion occurred due mainly to the collision of suspended sand particles against the pile surface. At the lower part of the sand bed surface, however, the pile underwent sliding abrasion caused by sand particles in a state of liquefaction.

The results of the experiments indicate that the collision energy of suspended sand particles affects the maximum amount of abrasion on the surface of a steel pile. To determine the collision energy of sand particles against the surface of the pile, numerical analysis of the motion of suspended sand particles was performed.

Fig. 6 shows a sketch of sand particle motion. It was assumed that the fluid flow in the front of a pile was a two-dimensional, steady, potential motion. The sand particle motion was determined by Eq. 1.

$$M \frac{d\bar{U}}{dt} + C_M m \frac{d(\bar{U} - \bar{u})}{dt} = m \frac{d\bar{u}}{dt} + \frac{1}{2} C_D \rho_w A |\bar{u} - \bar{U}| (\bar{u} - \bar{U}), \quad (1)$$

where M and m are the mass of the sand particle and the mass of water displaced by the sand particle, respectively;  $\bar{U}$  and  $\bar{u}$  are the velocity vectors of the sand particle and fluid particle, respectively; A is the cross-sectional area of the sand particle;  $\rho_w$

is the density of the fluid; and  $C_M$  and  $C_D$  are the virtual mass coefficient and the drag coefficient, respectively. From the study of Sawamoto (1979), we assumed  $C_M$  to be 0.5, and  $C_D$  was determined by Eq. 2.

$$C_D = 0.4 + \frac{24}{Re}, \tag{2}$$

where  $Re$  is Reynolds number. As we assume that abrasion of a pile occurs due to the collision energy of sand particles against the pile, dimensionless collision energy is defined as follows:

$$\text{Dimensionless collision energy} = \frac{CVn|\vec{U}|}{u_0^2}, \tag{3}$$

where  $\vec{U}$  is the collision velocity vector of sand a particle;  $Vn$  is the normal component of  $\vec{U}$  to the pile surface;  $u_0$  is the amplitude of main flow velocity; and  $C$  is the dimensionless number of collision particles, defined as the ratio of the volume flux of sand particles at a point far from the pile to the volume flux when sand particles collided with the surface of the pile.

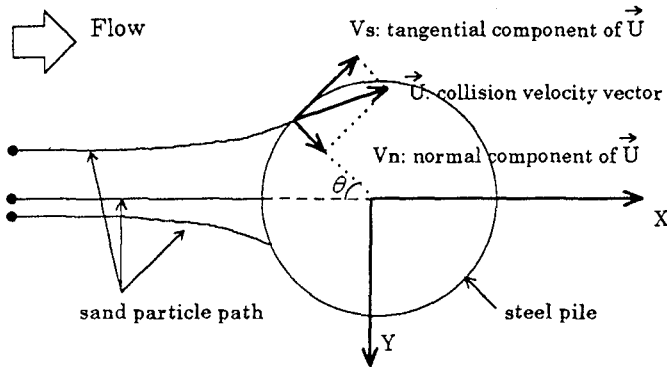


Fig. 6 Sketch of sand particle motion.

Fig. 7 shows the relationship between sand particle diameter, the calculated dimensionless collision energy, and the measured abrasion rate around a pile. Numerical analysis was carried out under the following conditions: flow velocity  $u_0$  and diameter of pile  $\phi$  were 3.0m/s and 30cm, respectively, and the diameters of sand  $d$  were 1, 4 and 10mm. Fig. 7 also shows the measured abrasion rates of steel piles of 267mm in diameter in a large U-shaped tube with sand of 7, 4, 1.5 and 0.75mm in diameter at a maximum flow velocity of 3.0m/s for 3 days. The horizontal axis  $\theta$  is the angle of the pile surface. The collision energy increased as the sand particle diameter increased. The collision energy of large sand particles was distributed over

a wider range of angles  $\theta$  compared with that of small sand particles. The rate of abrasion also increased as the diameter of the sand particles increased. The abrasion rate of large sand particles was distributed over a wider range of angles  $\theta$  than that of small sand particles. The collision energy distributions obtained by numerical analysis almost coincide with the distributions of measured abrasion rates.

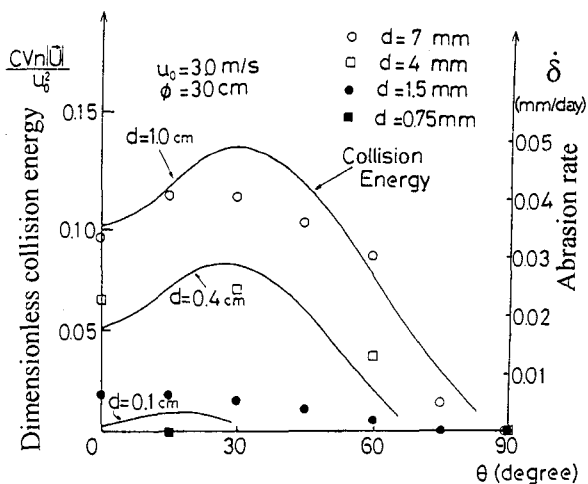


Fig. 7 Relationship between sand particle diameter, collision energy, and rate of abrasion around a pile.

Fig. 8 shows the relationship between sand particle diameter, maximum dimensionless collision energy, and maximum abrasion rate obtained from Fig. 7. The maximum collision energy of sand particles increased with increases in the sand particle diameter. The maximum collision energy was nearly proportional to the measured maximum abrasion rate.

Fig. 9 shows the relationship between pile diameter, dimensionless collision energy, and the rate of abrasion of the pile. The conditions for calculation were as follows: flow velocity is 3.0 m/s, sand particle diameter is 8 mm and pile diameters are 7.5, 10, 15, 30 and 100 cm. Fig. 9 also shows measured rates of abrasion of the steel piles of diameters of with 7.6, 14.0 and 26.7 cm under conditions in which the sand particle diameter is 7 mm and the amplitude of flow velocity is 3.0 m/s. The collision energy of the sand particles increased with decreases in the pile diameter. The collision energy of a small pile was distributed over a wider range of angles  $\theta$  compared with that of a big pile.

Thus, the larger the sand particle diameter and the smaller the pile diameter are, the higher the abrasion rate and the wider the abrasion area become. The reason for this is as follows. Fig. 10 shows an illustration of the collision behavior of sand particles and the streamlines of fluid near a pile without sand particles. When the diameter of

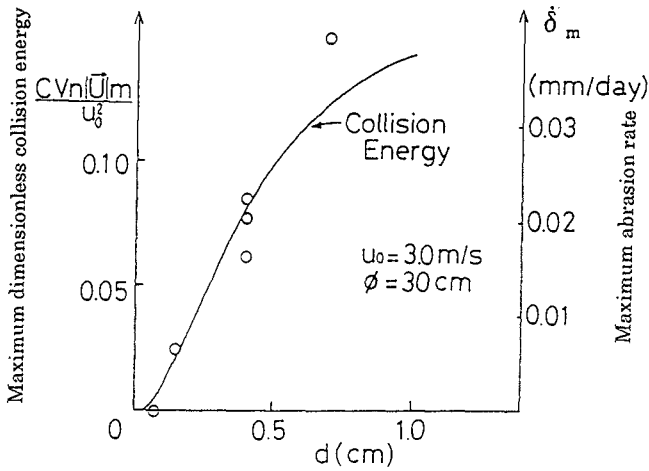


Fig. 8 Relationship between sand particle diameter, maximum collision energy and maximum abrasion rate.

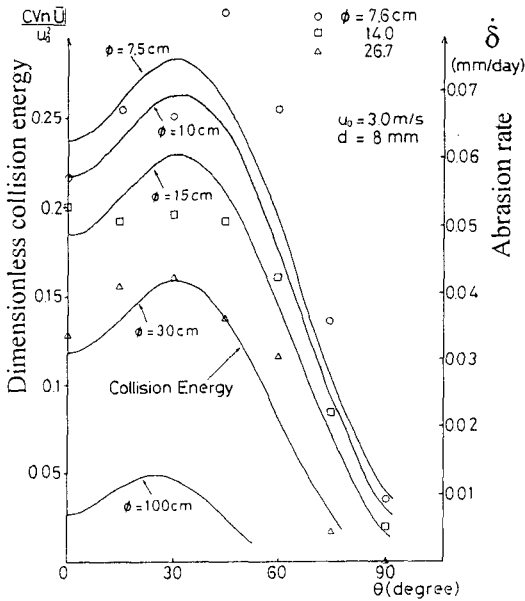


Fig. 9 Relationship between pile diameter, collision energy, and rate of abrasion around pile.



the sand particles is small, most of the sand particles tend to follow the fluid particles and do not contact with the surface of the pile because they have low inertia. Thus, the collision energy at the surface of the pile is very small. When the diameter of sand particles is large, however most of the particles collide with the surface of pile regardless of the flow of fluid around the pile, and thus the collision energy is very large. On the other hand, when the diameter of the pile is large, streamlines begin to curve at a point far away from the pile because of the pile's wall effect. When the diameter of pile is large, most of the sand particles closely follow the streamlines and do not contact with the surface of the pile due to the large wall effect.

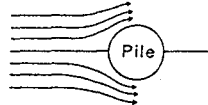
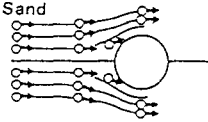
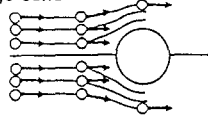
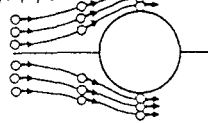
	Streamline without sand.
	Most fine sand follows the streamline without collision because it has low inertia. The energy transferred to the pile is low.
	Most large sand particles collide with the pile due to inertia. The energy transferred to the pile is high.
	Most sand particles follow the streamline without collision because of the large wall effect. The energy transferred to the pile is low.

Fig. 10 Illustration of the collision behavior of sand.

Fig. 11 shows the relationship between the ratio  $d/\phi$  of sand particle diameter to diameter of the pile and dimensionless maximum collision energy. The maximum collision energy is a function of only the ratio  $d/\phi$  approximately. The larger  $d/\phi$  is, the larger the maximum collision energy becomes.

Fig. 12 shows the relationship between  $d/\phi$ , maximum dimensionless collision energy, and maximum abrasion rate. The maximum abrasion rate is also a function of only the ratio  $d/\phi$  approximately. The collision energy obtained by numerical analysis is nearly proportional to the measured abrasion rate. This relationship is as follows. Dimensionless collision energy of 1.0 corresponds to an abrasion rate of 0.21mm/day at a flow velocity of 3.0m/s.

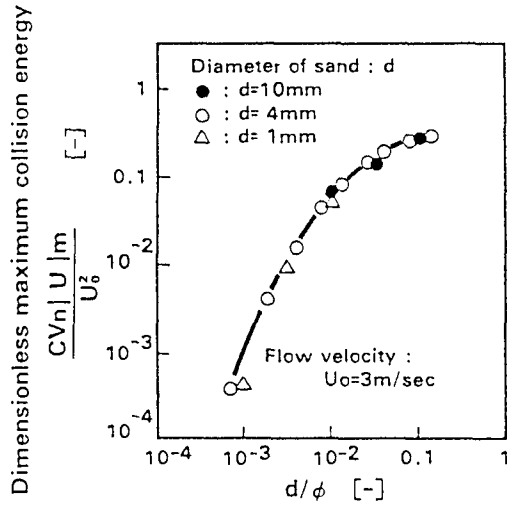


Fig. 11 Relationship between ratio of diameter ( $d$ ) of sand to diameter ( $\phi$ ) of pipe and dimensionless maximum collision energy.

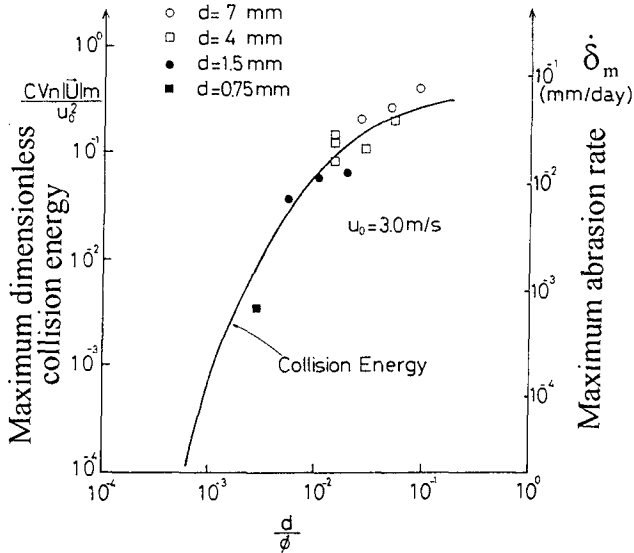


Fig. 12 Relationship between  $d/\phi$ , maximum collision energy, and maximum abrasion rate.

Fig. 13 shows the relationship between flow velocity, dimensionless maximum collision energy, and maximum abrasion rate. If flow velocity is larger than 1.0m/s,

the dimensionless maximum collision energy is nearly constant. The maximum abrasion rate is roughly proportional to the maximum collision energy. The rate of abrasion of a steel pile is roughly proportional to the second power of flow velocity.

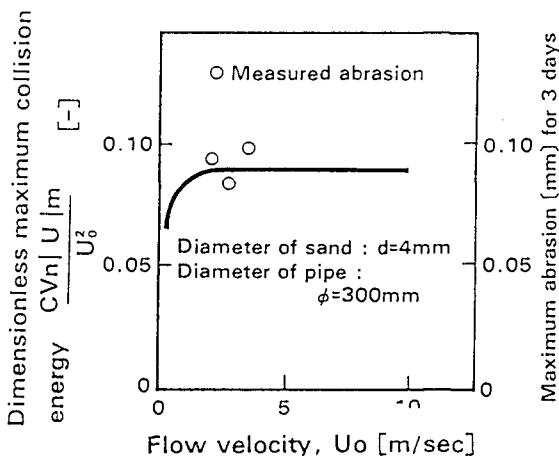


Fig. 13 Relationship between flow velocity and dimensionless maximum collision energy.

## CONCLUSIONS

The distributions of abrasion rate around and along steel pipe piles were clarified. The maximum abrasion rate was observed about 50mm above the sand bed and 15~30 degrees in the main flow direction. It is confirmed that an abrasion rate of 1mm/year can be expected in coastal zones with severe sand motion.

The abrasion rate of a steel pipe pile is roughly proportional to the second power of the amplitude of flow velocity.

The larger the sand particle diameter is and the smaller the pile diameter, the higher the abrasion rate becomes and the wider the abrasion area. This reason for this is as follows. When the diameter of sand particles is small and the diameter of the pile is large, more of the sand particles tend to follow the fluid particles and do not contact with the surface of the pile due to their low inertia and the large wall effect, respectively. The collision energy of sand particles obtained by this numerical analysis is nearly proportional to the measured abrasion rate.

The maximum collision energy is approximately a function of only the ratio  $d/\phi$  (sand particle diameter to pile diameter). The larger  $d/\phi$  is, the larger the maximum of abrasion rate and the maximum collision energy become.

As the relationship between collision energy and measured abrasion rate has been clarified, the abrasion rate can be estimated from the collision energy.

**REFERECES**

- Culbertson W.Ross(1949): Deterioration of Steel Sheet Pile Groins at Palm Beach, Florida, Corrosion, Vol.5, pp.339-342.
- Yamashita,T., H.Saeki, N,Asakawa, K.Sato and Y.Kariyazono(1989): Experimental Study on Abrasion of Steel Pile by Sediment Transport, Proceedings of Civil Engineering in the Ocean, JSCE, Vol.5, pp.109-112.(in Japanese)
- Yamashita,T., H.Saeki, Y.Senda, K.Sato and Y.Kariyazono(1990): Abrasion of Heavy Duty Anti-Corrosion Steel Pile due to Sand Transport under Oscillatory Flow, Proceedings of Coastal Engineering, JSCE,Vol.37, pp.394-398.(in Japanese)
- Yamashita,T., H.Saeki, Y.Senda, K.Sato and Y.Kariyazono(1991): Relation between Abrasion of Heavy-Duty Coated Steel Pipe and Collision Energy of Sand Particle due to Sediment Transport in Coastal Zone, Proceedings of Civil Engineering in the Ocean, JSCE,Vol.7, pp.231-236.(in Japanese)
- Yamashita,T., H.Saeki, Y.Senda, T.Someya, K.Sato and Y.Kariyazono(1992): The Effects of Sand Particle Diameter and Pile Diameter on the Abrasion Rate of Steel Pile by Littoral Drift, Proceedings of Coastal Engineering, JSCE, Vol.39, pp.481-485.(in Japanese)
- Kariyazono,Y., K.Sato, T.Yamashita and H.Saeki(1992): Abrasion of Heavy-Duty Coated Steel Piles by Sediment Transport in Coastal Zone, Proceedings of 1st International Conference of CORROSION ASIA' 92, pp.341-351.